Image motion and flexure compensation of the FORS Spectrographs

Harald Nicklas[a], Hermann Böhnhardt[b], Walter Fürtig[c], Reiner Harke[a], Achim Hess[b], Peter Jürgens[a], Bernard Muschielok[b], Walter Seifert[c], Otmar Stahl[c], Karl Tarantik[b]

[a] Universitäts-Sternwarte, Geismarlandstr. 11, D-37083 Göttingen, Germany

[b] Universitäts-Sternwarte, Scheinerstr. 1, D-81679 München, Germany

[c] Landessternwarte, Königstuhl, D-69117 Heidelberg, Germany

ABSTRACT

One of the most critical issues in designing a spectrograph is the motion of opto-mechanical components due to flexure especially when it will be mounted to the Cassegrain focus of a telescope. Image motion on the detector has to be kept small in order not to affect the value of the scientific data. The FORS spectrographs fulfil those requirements by a proper design and by a *passive* compensation of the instrumental flexure. Image motion of the 2 metric tons instrument could be reduced in this way to a tiny fraction of one pixel's size thus not affecting the data gathered with those spectrographs. It is tested and approved at a telescope simulator that all specifications regarding those motions are fully met. A fine tuning in flexure compensation is built into the spectrograph's design and is tested on its tuning range which allows to adapt the compensation to effects eventually caused by the Cassegrain flange of the telescope.

Keywords: optical instrumentation, focal reducer, spectrographs, image motion, flexure compensation, performance tests, verification

1 INTRODUCTION

The first of two copies of the **FO**cal **R**educer/**S**pectrographs of the Very Large Telescope (VLT) is extensively tested on all aspects of flexural behaviour of its critical components like the multi-object-spectroscopy unit (MOS), the individual slitlets, the dispersing elements as well as collimator and camera optics and CCD detector. The latter three components are responsible for image motion and possible data degradation in all observing modes. Testing this behaviour becomes one of the biggest issues at the telescope simulator especially in view of the passive flexure compensation which was calculated prior to construction.

We will show in the following that the *passive* flexure compensation works and that the FORS instruments meet the specifications for image motion on the detector to the tight tolerance of less than one quarter of a pixel during 1-2 hours of integration time. Effects of the telescope and its instrument attachment flange on the final image motion is discussed as well as the strategy to counteract those negative effects by the built-in fine tuning of the flexure compensation. This fine tuning is also tested on its sensitivity and its range which allows for last-minute changes in compensation by adapting the instrumental bending to the telescope's flange stiffness. Other aspects of structural stiffness, relevant for data quality e.g. in the spectroscopic mode, are well tested and will also be addressed. Tests on units and sub-units that

could be performed without a telescope simulator are already published [1] whereas the full performance specifications of the FORS spectrographs are given as design benchmarks [2].

2 TEST SETUP

All testings are performed by means of two simulators, a telescope and a star simulator. The telescope simulator (functional description in [1]) provides two-axis motion necessary to cope with all possible aspect angles of the instrument with respect to the gravity vector. Tracking on stellar objects leads for a Cassegrain instrument (independent of equatorial or alt-az mount) to the full range of gravitational load vectors of the entire sphere considering push and pull forces as the same load. The 3-metre instrument of more than 2 metric tons weight was bolted to the simulator flange and slewed into all orientations that are possible during observation (Fig. 1). The data are primarily taken with two procedures in order to cover the full operational range; a) rotating the instrument two full turns (forward and backward) when pointing to 30°, 60°or 80°zenith distance (ZD), b) slewing the instrument by ± 80°from the zenith for two position angles of 90°separation i.e. slewing it from east to the west and from the north to the southern horizon respectively. The image motion of all other aspect angles can in principle be modelled from the parameters obtained in that way.

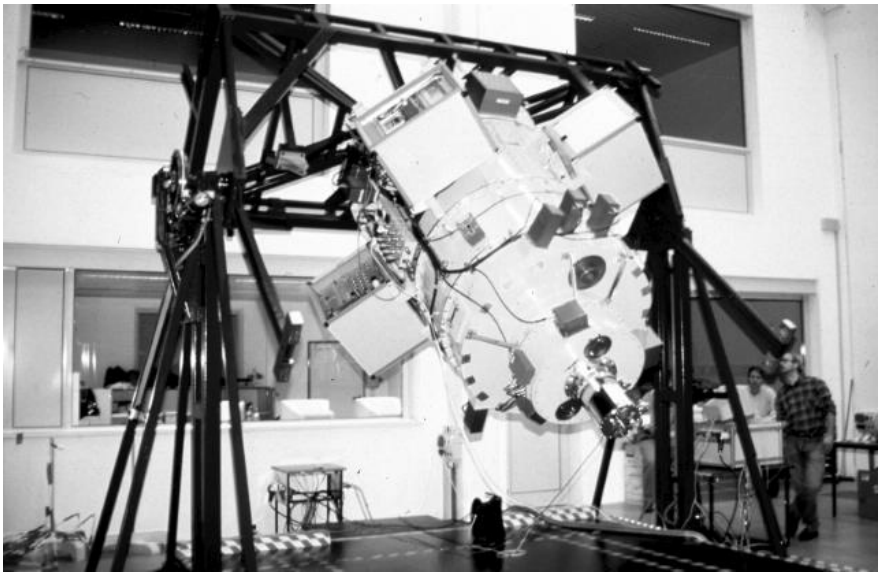

Figure 1: The FORS-1 spectrograph mounted to the telescope simulator during flexure testing in the integration hall at DLR/Oberpfaffenhofen. All functions of the instrument, the telescope and the star simulator can be remotely controlled from the control room in the back.

The star simulator projects stellar images with the f-number of the telescope into the instrument for image quality and straylight assessment and illuminates the pinholes that are inserted into the focal plane common to the instrument and the telescope. Two kinds of pinholes are provided for those tests; a) an internal pinhole, mounted inside of the instrument into the longslit mask thus reflecting any image motion caused by the instrument itself and b) an external pinhole, bolted to the simulator flange in order to assess effects which are caused by the attachment flange. The external pinhole was tested before on their intrinsic stiffness to ensure that it can be considered as sufficiently stable regarding bending motions which become important in detecting flange effects.

Further tests covering other opto- and electro-mechanical aspects and software tests of the FORS spectrographs that were performed with the telescope and star simulators are given in a separate paper of this conference [3].

3 IMAGE MOTION AND FLEXURE COMPENSATION IN DIRECT IMAGING MODE

Mechanical flexure which normally affects the stability of the opto-mechanical components within the light path can be used to compensate its negative image shifts by a proper design. A kind of *passive* compensation uses the fact that an image shift caused by a translation of a collimator can be compensated by tilting the imaging camera by an appropriate amount. The flexure compensation built into the FORS spectrographs can use earth's gravity because translation and tilt of the optical components has to go in the same direction in order to counteract. The challenging issue of such compensation is to design a mechanical structure of appropriate stiffness for the involved opto-mechanical components, mainly the collimators, camera and the detector dewar. The mechanics design of the FORS spectrographs is being cast into a computer model in order to estimate and manufacture the right ratio in stiffness of those parts. Those computations cover extensive finite-element (FE) analyses and ray tracings in the course of which the model and the design evolved to its final state in which the resulting image shifts on the detector could be reduced down to the one-micron level. This theoretical value had to be verified for the two collimators of different focal length.

A second issue of the FE analysis of the opto-mechanics was the development of a fine tuning of the stiffness ratio between collimator translation and camera tilt. The analysis turned out that the area which reacts most sensitive to that kind of manipulation is a recess in diameter of the cylindrical housings of FORS. Such a diameter change was designed into the filter/camera section and re-stiffened by diagonals in such a way that the final tilt of the camera itself could be adjusted within a specific range by size, position and number of those diagonals. That computed range of tilt variation had to be verified at the telescope simulator too.

3.1 Image motion of the instrument

The first assessment on image motion covered the shifts that are caused by the instrument itself without any external contribution. These measurements were performed with an internal pinhole of the spectrograph which gave the residuals of image motion that remain on the detector after flexure compensation. The pinhole images are taken with the CCD and their center position is determined using MIDAS. Those center positions are plotted to scale for each pointing of the instrument starting at the zenith with a slew to the observation altitude and one or two full turns of 45°step size at constant attitude. The circles of image motion are generally taken at zenith distances of 60°, 80°and 30°. The re-stiffening of the effective camera tilt by different numbers of diagonals attached to the filter/camera section becomes an additional parameter in the tests.

The first set of image motion circles is taken with the collimator of the standard spatial resolution mode (SR) within the light beam. Those residual motions are plotted to scale in Figure 2 for different setup of 0, 10 and 18 diagonals. A reduction in image spread from 5 pixel diameter to less than 1 pixel radius at 60°ZD is gained by increasing the stiffness at the filter/camera section to the maximum number of 18 diagonals. In case of the exchangeable collimator of the high spatial resolution mode (HR), the diameter of image motion is reduced by a factor of two compared to the SR mode. In Figure 3, the circle of 4.5 pixel diameter for the weak configuration without diagonals (U00) reduces to a circle of less than 0.5 pixel radius for the stiffest setup (U18) in the HR mode.

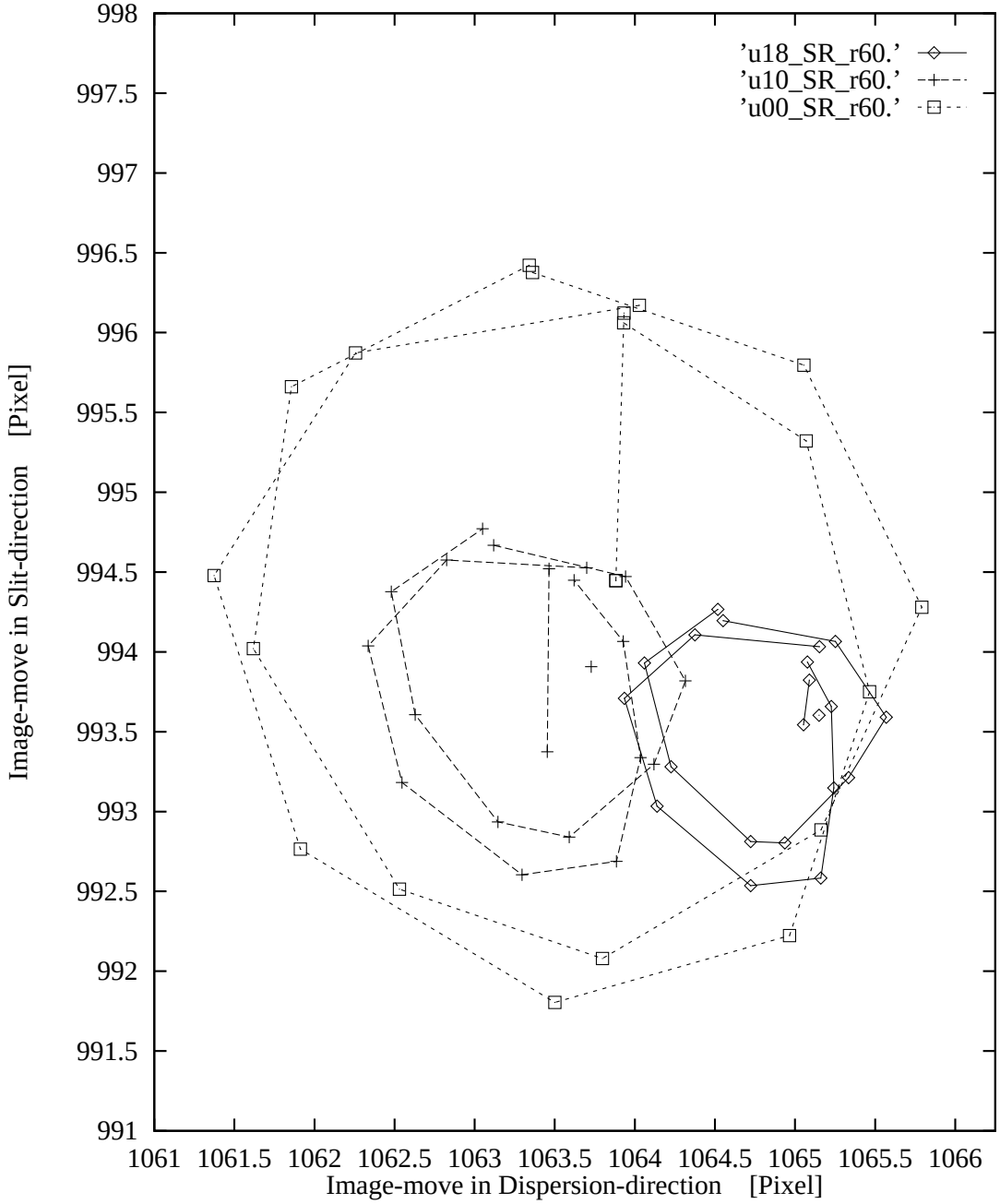

Figure 2: Residual image motion on the CCD for an *internal* pinhole after flexure compensation. The plots are an excerpt out of dozens of images taken with the collimator of the standard spatial resolution mode (SR). The number of diagonals vary from maximum (U18) to minimum stiffness (U00) as parameter. The image motion circles are taken by full turns at 60°zenith distance. The slew from zenith to the altitude is also visible. The offset in centring is due to de- and re-attachments of collimator, camera section and CCD cryostat as well as collimator exchange between exposures.

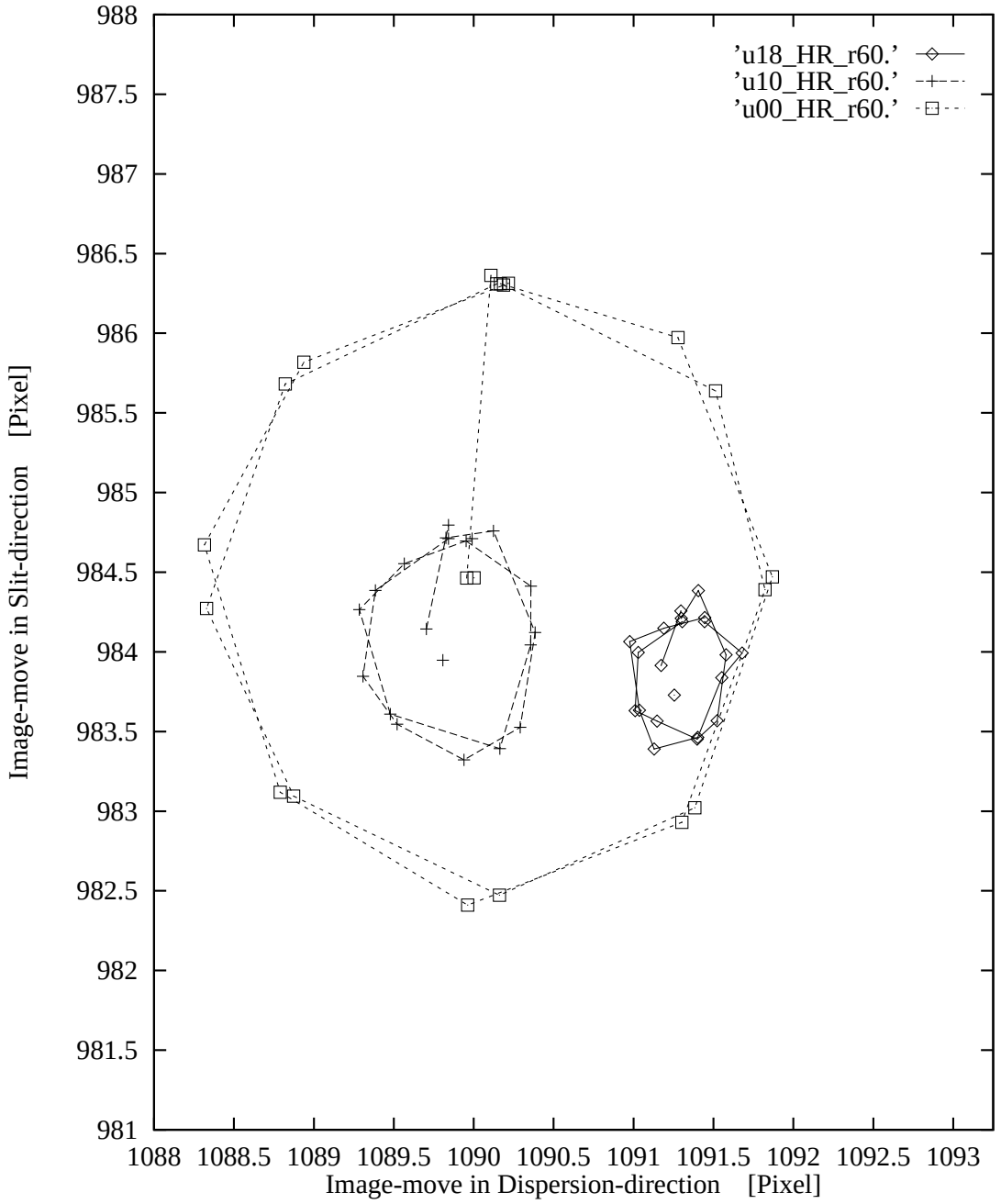

Figure 3: Residual image motion on the CCD for an *internal* pinhole after flexure compensation. The graphs are a representative sample of images taken with the collimator of the high spatial resolution mode (HR). The number of diagonals vary from maximum (U18) to minimum stiffness (U00) as parameter. The image motion circles are taken with the same procedures as those in SR mode of Figure 2. The decenter is for the same reasons.

The two major axes of the image motion circles are drawn in Figure 4 for the extreme cases of minimum and maximum stiffness in both imaging modes, standard and high resolution. The radii follow (closely) a sine-function in zenith distance which was expected due to the effective gravity force acting on the structures according to Hooke's law. The weak configuration without any diagonal re-stiffening fits with a sine-amplitude of 2.5 pixel in SR and about 2 pixel in HR mode. Those amplitudes reduces for maximum stiffness (18) and minimal camera tilt to approx. 1 pixel in SR and 0.5 pixel in HR imaging mode.

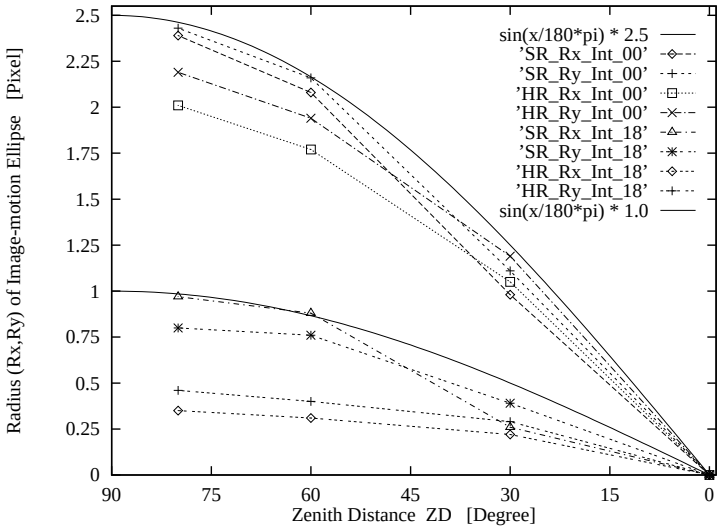

Figure 4: Dependence of the image motion on zenith distance for the two observing modes, imaging with standard and high spatial resolution (SR, HR). Given are the two major axes (Rx, Ry) of the image motion circle of an internal pinhole at minimum stiffness in the upper curves and at maximum stiffness of 18 diagonals in the lower graphs. All scale closely with $sin(ZD)$ according to Hooke's law. The single deviation at 30°ZD is an underestimate due to an incomplete run. The lower curves at maximum stiffness are in compliance with the quarter pixel specification of image motion for 1 and 2 hours integration time respectively.

The residual image motion for the FORS spectrograph itself at any aspect angle can thus simply be modelled by $1.0 pixel \times sin(ZD)$ in standard and $0.5 pixel \times sin(ZD)$ in high resolution imaging mode. Any shifting of a point image for a given exposure time can then be calculated by taking the difference between the corresponding altitude angles taking into account the change in position angle if necessary. From the point of view of instrumental flexure alone, the FORS spectrographs are already within the specification of a quarter pixel shift for one and two hour integration in SR and HR mode respectively. For high resolution observations of up to 30°zenith distance, flexure compensation will keep the spectrograph 24 hours within the quarter pixel specification.

3.2 Image motion covering external effects

Separate test runs were performed to figure out the influence of external effects like stiffness of the attachment flange on image motion. An 'external' pinhole was therefore mounted to the simulator flange which should represent a stable image within the focal plane of the telescope. A shift in image motion radii could be observed when changing from internal to the external pinhole. Those image motion circles (for internal and external pinhole) are plotted for comparison in Figure 6 for a constant setup of 10 stiffening

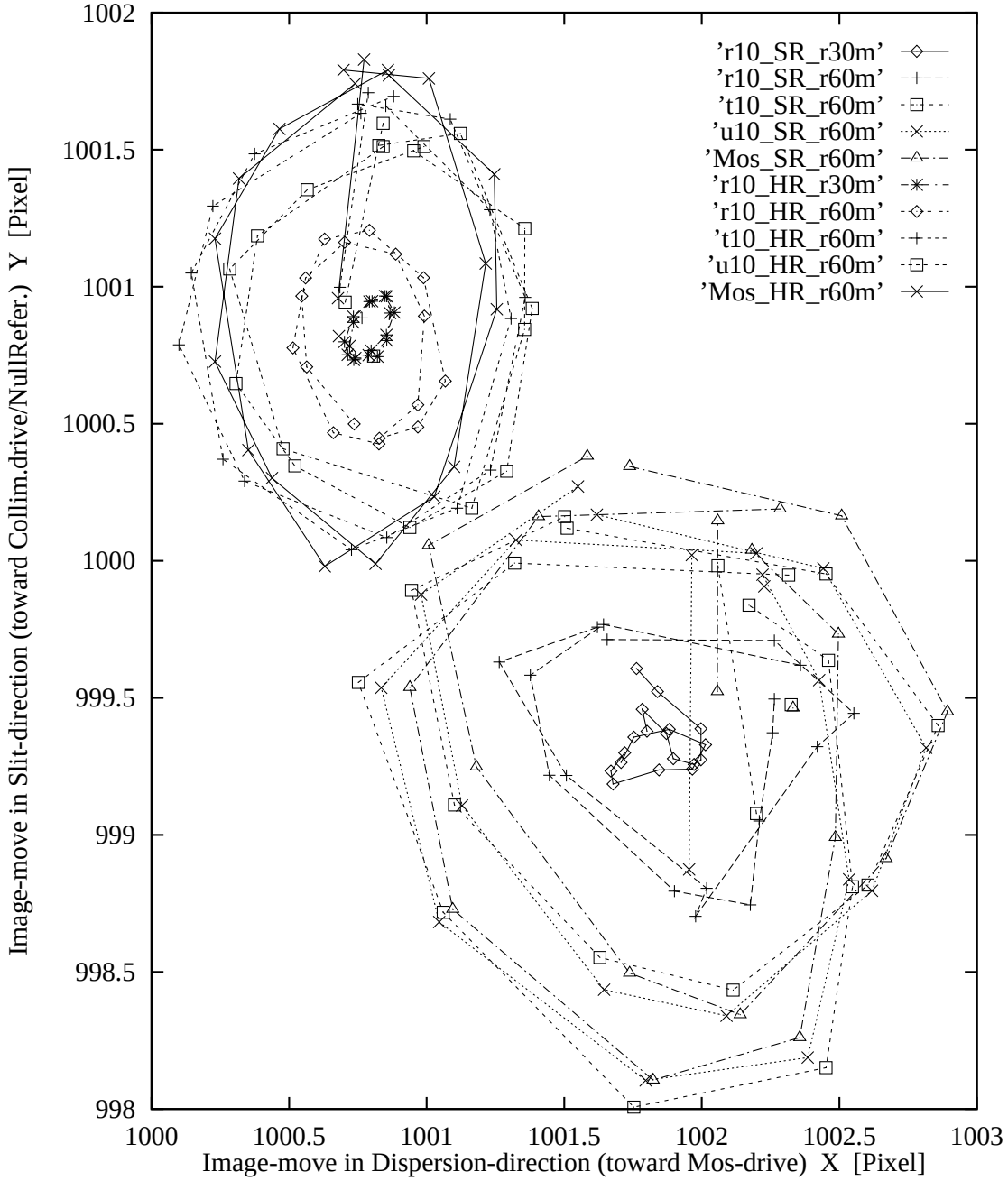

Figure 5: Residual image motion in both modes, standard (SR) and high spatial resolution (HR) imaging, for both pinholes, internal (t10, u10 and MOS) and external (r10), and a constant setup of 10 diagonals. Each circle is shifted for comparison purposes to a common center at lower right for SR and upper left for HR mode. The similar shape of the circles for each mode is obvious. Also the scaling with zenith distance (r30°, r60°) and with flange stiffness (r10 *with*, t10, u10 and MOS *without* flange effect) can be seen.

diagonals. The shift in the standard resolution mode becomes visible when comparing the curves of the internal pinhole (u10_SR and t10_SR) with that of the external pinhole (r10_SR) at 60°zenith distance. One observes a decrease of about a factor of two in diameter. The same is true for the high resolution mode where the circles for the internal pinhole (u10_HR and t10_HR) decrease to about 0.5 pixel diameter (r10_HR) for an external pinhole mounted to the attachment flange. It shall be pointed out that a close inspection of that rotation curve reveals a change in sign. This corresponds to a switch from over- into under-compensation which means that the tilt of the camera is not large enough to fully compensate the larger image shift produced by the high resolution collimator with its two times shorter focal length with respect to the standard collimator.

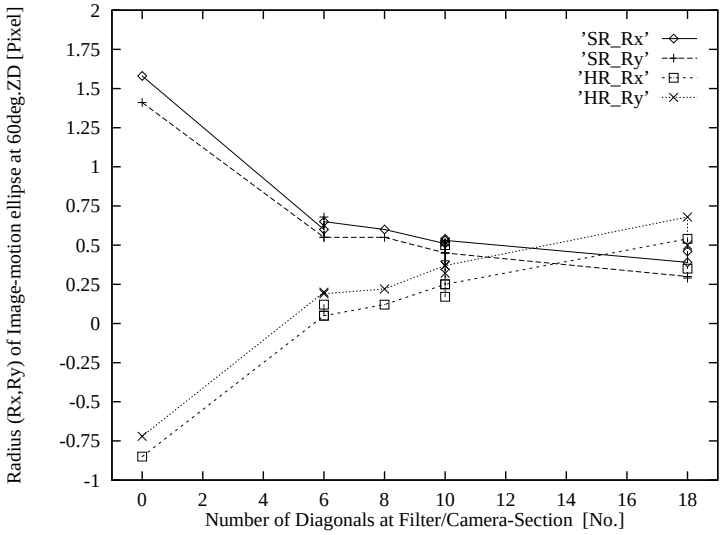

Figure 6: The radius of the two major axes (Rx, Ry) of the image motion circle as function of the number of stiffening diagonals. The image motion is taken with the external pinhole thus including flange effects. The relation is linear until the turn-off point where re-stiffening disappears and push-pull forces are replaced by bending.

The spread in radii of the image motion circles as a function of diagonals re-stiffening and reducing the camera tilt is plotted in Figure 6. The relationship is quite linear until the turn-off point is reached when all diagonals are removed and the tilt of the camera experiences a discontinuous increase due to the fact that the main loads of the camera housing changes from push-pull forces into a bending momentum. It becomes obvious from Figure 6 that the optimal flexure compensation for *both* imaging modes (SR and HR) is a compromise between over-compensation in one mode and under-compensation in the other since the linear relation is running diametrically for the two modes. Thus, the best compromise between both imaging modes would be a residual circle of equal radius but opposite compensation. The symmetrical configuration of re-stiffening diagonals which falls closest to that requirement is that of 10 diagonals. The radius of image motion of an external pinhole would then amount to about 0.5 pixel in the SR and 0.25 pixel in the HR mode for observations of up to 60°zenith distance. It has to be pointed out, that those statements are only valid for attachments which are comparable in stiffness to that of the simulator flange. Any deviation from that stiffness will change the properties which will be addressed in the following discussion on flange stiffness.

4 FOCAL PLANE MOTION AND FLANGE EFFECTS

The stability of the focal plane with respect to the simulator flange was measured in a separate test run. An electronic gauge was mounted for that purpose to the central part of the simulator flange. The mount also contained an illuminated pinhole in order to cross-check the residual image motion compared to that measured with the external pinhole. The circles of residual image motion at horizontal pointing are identical for both setup. Those test runs support the confidence regarding stability of instrumental flexure and of both external pinholes which are independently tested on their stability.

The gauge sensors are mounted within the focal plane of the instrument in order to detect any motion of the multi-object-spectroscopy (MOS) unit itself as well as of an individual slitlet of the MOS. The gauges sense two different motions belonging to those parts (Fig. 7). The motion detected at the MOS unit (Focl) representing the instrumental focal plane formed perfect circles at all zenith distances corresponding to 45 μm radius at 90°ZD. Slews to opposite horizons are performed additionally for detailed checking of the relationship to zenith distance which followed perfectly a sine-function within 1 μm . We found that this motion of 45 μm amplitude does not belong to the MOS unit but to the simulator flange as a detailed FE model of the flange revealed. A bending of the outer structure of the simulator flange tilts the entire instrument leading to a shift of the focal plane with respect to the optical axis. The final minimization of image motion therefore requires the real attachment of FORS to the actual telescope flange. Presently, only assumptions on the flange stiffness regarding instrumental load can be made. Taking into account the finite stiffness of the telescope flange and the relation of structural properties to the simulator flange one could expect a stiffness of the telescope flange twice as big leading to instrumental tilt and motion of the focal plane of roughly half that amount i.e. some 20 μm amplitude. This value corresponds quite well with an indicative estimate done with a model of the Cassegrain Adapter/Rotator of the VLT unit telescope. Taking into account that amplitude which can not be distinguished from intrinsic instrumental image motion, the residual motion shifts closer to the optimum of over-compensation in SR and under-compensation in HR mode as it is discussed above. Although specifications are already met for an infinitely stiff flange, the final flexure compensation will produce image motion of only a fraction of the quarter-pixel specification for the flange stiffness that is to be expected.

Nevertheless, if it would become necessary at the telescope, more re-stiffening can be gained by increasing the cross-section of the diagonals which carry about 3/4 of the bending load applied at the filter/camera section. Thus we have the opportunity to shift the designed tuning range into the regime required by the telescope flange.

The total motion of any equipment (e.g. masking devices) within the focal plane amounts to less than 10 μm within the instrument reference frame. This corresponds to 0.″02 (i.e. 0.1 pixel) image motion from zenith to the horizon which is negligible for reasonable exposure times. This value calculated by FE computer modelling is in excellent agreement with the amount measured in special hardware tests in the course of which the attachment of the instrument was simulated and a momentum of 20 kNm was applied to the housing of FORS-2. All displacement values gathered so far at the telescope simulator, in the attachment simulation and FEA modelling are conform with each other.

The individual slitlets are also tested on their stability within the focal plane. They exhibit an elongated circle (*Slit* in Figure 7) distorted by the bending of the slitblade carrier. The circular motion (*Focl*) caused by the simulator flange has to be subtracted. The remaining slitlet motion with respect to the focal plane amounts to 7 μm in dispersion direction and 57 μm along the slit corresponding to 0.″01 and 0.″1 respectively when slewing from zenith to horizon. This does not contribute significantly to image motion as shown by the motion circles (MOS) in Figure 5 taken directly with slit images of the MOS.

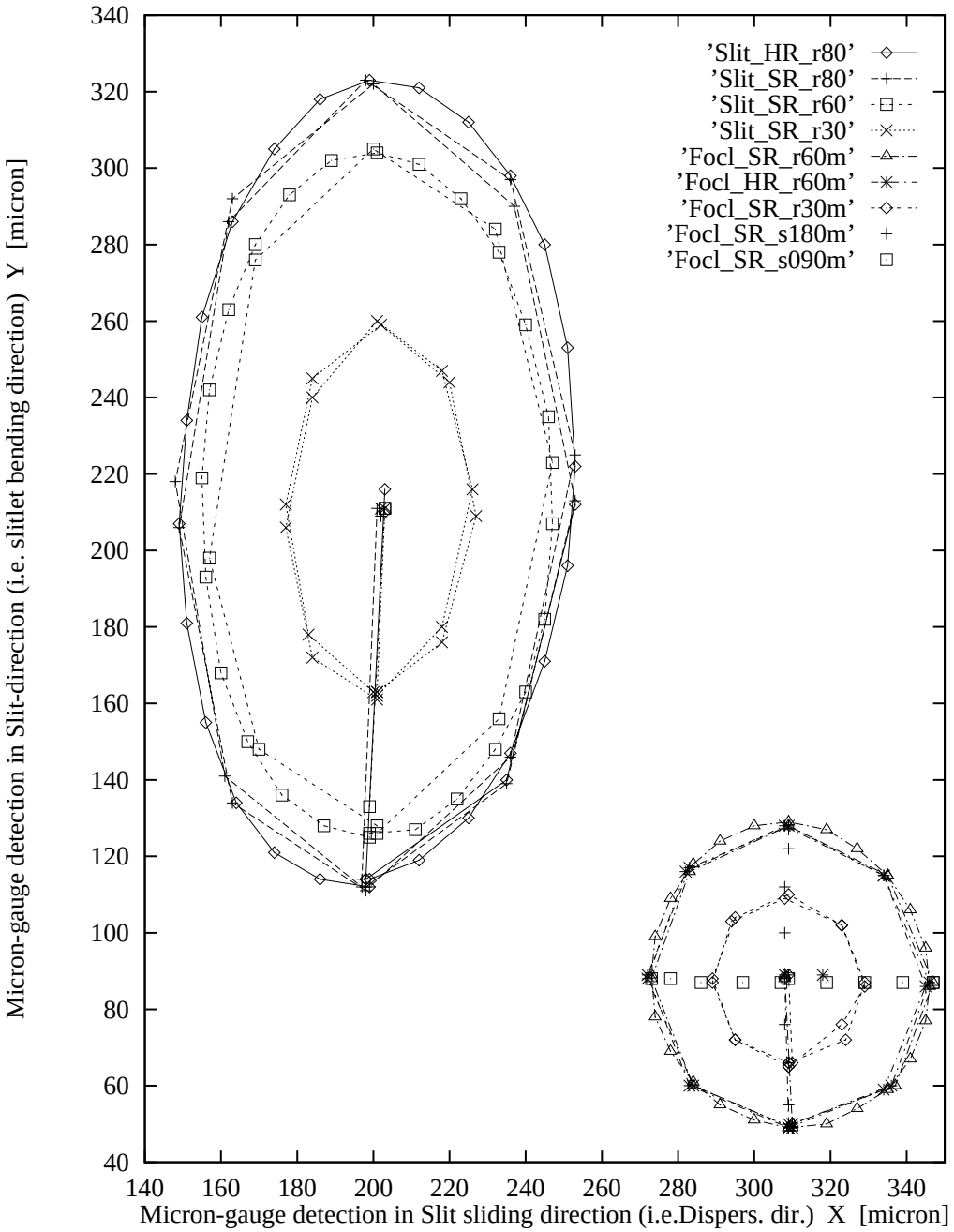

Figure 7: Translations of the focal plane and individual slitlet. It is detected directly by an electronic gauge mounted within the focal plane with attachment to the flange of the telescope simulator. The lower right circles (Focl) of MOS motion, representing the focal plane, are caused by deformations of the simulator flange tilting the entire instrument. The motion of the individual slitlet (Slit) is superpositioned onto that perfect circle with an enlargement in Y. That additional translation is produced by bending of the slitjaw carrier but will not affect the scientific data due to its direction along the slit and the keeping of slit parallelism specification.

A close inspection revealed some minor hysteresis in Y of the gauge sensing (*Slit* of Figure 7) which is caused by the bending momentum acting on the linear motion guides of the individual slitlets. This hysteresis is not of concern due to the small value and its direction observed only along the slit. The translation of 57 μm along the slit due to bending was expected and exceeds the FE result by some 50 % due to imperfections in modelling the linear guides. That kind of hysteresis can also be observed for the two collimators which are exchanged by similar linear motion guides. It becomes visible by a small turn in position angle of the twin-circles of e.g. U10_SR and U10_HR in Figure 5. This effect was investigated in more detail and turned out to be fully reproducible.

5 IMAGE STABILITY IN SPECTROSCOPIC AND POLARIMETRIC MODE

When switching from imaging into spectroscopic mode, one additional optical component contributes to the image motion. The stability of the dispersing elements, the grisms in case of the FORS spectrographs, within the beam is checked via shifts of the spectra on the detector. For that purpose, three out of seven grisms were inserted into the parallel beam in order to detect any possible tilt of the grism wheel or of the mount by those elements. The measurements determined the relative shift of spectra with respect to a reference exposure. The reference exposures are taken with identical slewing procedures as the measurements with the spectroscopic and polarization optics in the light path. The image motion was measured for each part of the analysis optics relative to the image position at the zenith. The instrument was slewed from zenith to 60°ZD and performed from that position $\pm$90°turns (forward and backward) in position angle. The inner accuracy of those measurements is checked by reproducing the reference point at the start of the measurements and is about 0.02-0.03 pixel.

The relative shift of the spectra falls within 0.03-0.05 pixel which is near to the limit of the measurement. The tilt of dispersing optics within the parallel beam could therefore be derived to less than 1 arcsec. The three exchange wheels containing the grisms, broadband-filters and the Wollaston prism can thus be considered as very stiff with respect to the parallel beam.

The polarisation optics comprising a Wollaston prism and two retarder-plate mosaics is tested in the same way as it is done for the grisms. Inserting the Wollaston prism and the $\lambda/2$ retarder plate into the parallel light beam revealed a shift of a point image of less than 0.03 pixel relative to the reference image taken at the zenith. The measurement for the $\lambda/4$ retarder plate together with the Wollaston prism is also close to the intrinsic uncertainties. The resulting tilt of about 1 arcsec is of the same order as it is estimated for the grism and belongs to the Wollaston prism since the phase-retarder mosaics are planeparallel plates. The correspondence of those tilt values was expected since both wheels, the Wollaston and the grism exchange wheel are placed on identical instrumental structures.

6 CONCLUSION

We have shown that flexure compensation is predictable, it works and can be utilized with a proper design. It is a *passive* compensation which can not fail when it is well designed and once adjusted after manufacturing. It is therefore recommended to build a tuning opportunity into the design. The quarter-pixel specification regarding image motion residual to the flexure compensation is met for all observing modes, for internal as well as external flexure of the instrument and structures respectively. Some measurements and computations indicate that we will finally obtain image motions of only a fraction of a quarter-pixel at the telescope.

We can claim that we understand the spectrograph's behaviour and that we own a good and precise theoretical model. This model is fully consistent in itself and with the wide variety of measurements taken so far. We are able to predict the displacement and tilt of the relevant parts of the opto-mechanics for all orientations and positions on the sky. Therefore, we will ship the instruments to the telescope with lowest uncertainties regarding flexural behaviour and with high confidence since we are able to adapt the final image motion to the stiffness of the flange which we will face at the telescope.

ACKNOWLEDGEMENTS

The FORS-Project is performed under ESO Contract 37548/ESO/VLT/91/7844/GWI and is supported by the *German Federal Ministry of Education, Science, Research and Technology* with grants 05 3GO10A, 05 3HD50A and 05 3MU104.

References

[1] H. Nicklas, H. Böhnhardt, S. Kiesewetter-Köbinger, W. Seifert, G. Rupprecht: "Construction of the FORS Focal Reducer/Spectrographs: Status report and first test results", in 'Optical Telescopes of Today and Tomorrow', A. Ardeberg (Ed.), SPIE Proc. **2871**, p.1222, 1997

[2] H. Böhnhardt, S. Möhler, H.-J. Hess, S. Kiesewetter, H. Nicklas, H.: "Design Benchmarks of the FORS Instrument for the ESO VLT", in 'Scientific and Engineering Frontiers of 8-10m Telescopes', Eds. M. Iye, T. Nishimura, Universal Academic Press, Tokyo, 1995

[3] T. Szeifert, I. Appenzeller, W. Fürtig, W. Seifert, O. Stahl, H. Böhnhardt, W. Gässler, R. Häfner, H. Hess, K.H. Mantel, W. Meisl, B. Muschielok, K. Tarantik, R. Harke, P. Jürgens, H. Nicklas, G. Rupprecht: "Testing FORS - the First Focal Reducer for the ESO VLT", in 'Astronomical Telescopes and Instrumentation', SPIE Proc. **3355**, this proceedings